Front. Environ. Sci. Eng. 2020, 14(4): 63
https://doi.org/10.1007/s11783-020-1242-0

RESEARCH ARTICLE

Transport of bacterial cell (*E. coli*) from different recharge water resources in porous media during simulated artificial groundwater recharge

Wei Fan, Qi Li, Mingxin Huo, Xiaoyu Wang, Shanshan Lin (✉)

School of Environment, Northeast Normal University, Changchun 130117, China

HIGHLIGHTS

- The recharge pond dwelling process induced changes in cell properties.
- Cell properties and solution chemistry exerted confounding effect on cell transport.
- *E. coli* cells within different recharge water displayed different spreading risks.

ARTICLE INFO

Article history:
Received 26 November 2019
Revised 24 February 2020
Accepted 26 February 2020
Available online 10 April 2020

Keywords:
Artificial groundwater recharge
E. coli
Transport
Simulated column experiments
Modeling

GRAPHIC ABSTRACT

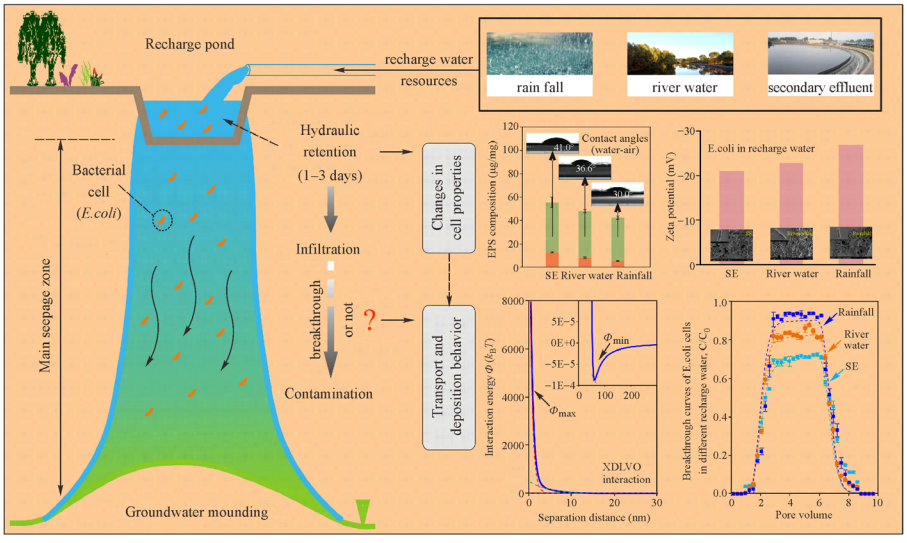

ABSTRACT

Commonly used recharge water resources for artificial groundwater recharge (AGR) such as secondary effluent (SE), river water and rainfall, are all oligotrophic, with low ionic strengths and different cationic compositions. The dwelling process in recharge pond imposed physiologic stress on *Escherichia coli* (*E. coli*) cells, in all three types of investigated recharge water resources and the cultivation of *E. coli* under varying recharge water conditions, induced changes in cell properties. During adaptation to the recharge water environment, the zeta potential of cells became more negative, the hydrodynamic diameters, extracellular polymeric substances content and surface hydrophobicity decreased, while the cellular outer membrane protein profiles became more diverse. The mobility of cells altered in accordance with changes in these cell properties. The *E. coli* cells in rainfall recharge water displayed the highest mobility (least retention), followed by cells in river water and finally SE cells, which had the lowest mobility. Simulated column experiments and quantitative modeling confirmed that the cellular properties, driven by the physiologic state of cells in different recharge water matrices and the solution chemistry, exerted synergistic effects on cell transport behavior. The findings of this study contribute to an improved understanding of *E. coli* transport in actual AGR scenarios and prediction of spreading risk in different recharge water sources.

1 Introduction

Artificial groundwater recharge (AGR) is a promising method for the addition of water to aquifers for various purposes such as short-term storage, wastewater recovery,

✉ Corresponding author
E-mail: linpapersubmit@163.com

improving water quality, depleted aquifer recharge, or the prevention of saline intrusion and ground subsidence (Bouwer, 2002; Zhu et al., 2019). AGR can be performed using a variety of water types including river water, storm water and treated sewage, such as secondary effluent (SE) (Dillon, 2005). While AGR offers significant potential benefits, the risk of migration of percolated exogenous contaminants from recharge wells or spreading ponds, presents the possibility of groundwater quality deterioration (Asanoa and Cotruvo, 2004). One particular concern associated with the safety of AGR is the risk of contamination with pathogenic microorganisms (e.g., coliforms), especially in scenarios involving recharge with raw water, wastewater or low level treated sewage (Levantesi et al., 2010) where *E. coli* is often detected at high concentrations (Amimi et al., 2014; Lopez-Galvez et al., 2016; Zhu et al., 2019). Considering the potentially widespread occurrence of *E. coli* and its use as a representative indicator of the microbial quality of water (Chen et al., 2018; Sherchan et al., 2018), a thorough understanding of the behavior of *E. coli* during seepage, is important to assess the environmental risks of AGR.

Previous bacterial transport studies have commonly considered specific environmental factors under controlled simulated conditions, using artificial controlled background solutions; and there have also been several studies investigating the transport and survival of microbes under natural conditions in field scale assessments (Foppen and Schijven, 2006; Pachepsky and Shelton, 2011; Dwivedi et al., 2013). These studies have revealed the bacterial retention mechanisms, including attachment to sand surfaces (saturated) or the three-phase interface (unsaturated), filtration through small pore channels or interception in water films (Engström et al., 2015; Madumathi, 2017). The specific effect of typical environmental variation on microbial transport in porous media has been clarified and colloid filtration theory has commonly been used to explain their transport and retention mechanism (Goldberg et al., 2014). It has been reported that the migration and deposition of viruses and bacteria in porous media occur as a function of hydrodynamic conditions, solution chemistry, surface properties of cells and sand, and concomitant organics/particles (Tong et al., 2010; Cai et al., 2013; Bradford et al., 2015). There is significant variation in the physicochemical conditions (such as pH, ionic strength (IS)) and coexisting dissolved organic matter of recharge resources in AGR such as rainfall, river water and SE. Therefore, the transport variability of bacteria in different real recharge water matrices from practical AGR applications needs to be fully elucidated by horizontal comparison, to assess the spreading risk of bacteria under different recharge scenarios.

In addition, the dwelling time of recharge water containing *E. coli* in the spreading pond, can range from several hours to days before cells enter the seepage zone (Kallali et al., 2013), allowing the onset of antecedent growth processes in *E. coli* when present in oligotrophic recharge ponds. As bacterial adhesion is related to the cells physiologic status and cell surface properties (Hori and Matsumoto, 2010; Mauter et al., 2013), the influence of this proposed antecedent growth scenario on *E. coli* transport during recharge water seepage is of critical importance. However, research on this mechanism under real-world AGR conditions has been largely neglected. Therefore, the objectives of this study were to (1) establish how the antecedent growth process alters characteristics of *E. coli* under environmentally realistic conditions; and (2) examine the transport behavior of *E. coli* through saturated porous media with different real recharge water types (rainfall, river water and SE), Simulated column experiments were performed to assess the transport behavior of *E. coli* based on breakthrough curves (BTCs) and retention profiles. Cell surface characterization, particle interaction calculations and transport numerical modeling were performed to provide detailed insights into the mechanisms of cellular transport and retention.

2 Materials and methods

2.1 Porous medium

Quartz sand (Sinopharm Chemical Reagent, China) sieved into 0.36–0.50 mm size particles was selected to simulate sand medium in the AGR system, with the average diameter being around 0.44 mm. Sand grains were angular shaped and were mainly composed of Si (37.85%) and O (62.15%) (FEI Co., Hillsboro, OR, USA) (See Fig. S1 in Supplementary Material). Sand particles were sequentially cleaned using tap water, 10% nitric acid (v:v) and deionized (DI) water, to remove impurities and obtain stabilized chemical properties. Then the material was dried at 80°C and sterilized by ultraviolet treatment (Wang et al., 2018).

2.2 Recharge water resources

Three types of recharge water were selected for investigation, rainfall, surface water from Yitong River and SE from a wastewater treatment plant (WWTP) in Changchun, Jilin Province in July 2018. To avoid biological interference in subsequent experiments, all water samples were filtered twice through filter membranes (0.22 μm) (MSM2008, Mosu Company, China) to remove suspended matters (including microbes) from samples. The main properties of the recharge water samples are presented in Fig. 1, which are similar to those reported by Wang (2012). The pH values of the three types of recharge water were in the range of 7.05–7.68. The TOC and COD values were 0.28±0.04 and 2.47±0.13 mg/L for rainfall, 5.25±0.68 and 10.37±0.71 mg/L for river water, and 7.53±1.02 and

18.43±0.83 mg/L for SE. The corresponding average IS values were calculated to be 0.35, 4.87 and 7.66 mM using the method described in Jalšenjak (2006). Three-dimensional excitation-emission matrix (3DEEM) analysis was employed to evaluate the fluorescence properties and the structure of dissolved organic matter in different recharge water matrices, at excitation wavelengths from 220 to 450 nm and emission wavelengths from 280 to 550 nm, at 5 nm intervals (LS-55, PerkinElmer, USA) (Chen et al., 2003; Hao et al., 2012). Detailed analyses of the 3DEEM speactra and fluorescence regional integration (FRI) are outlined in S1 in the Supplementary Material. As shown in Fig. 1, the distribution of fluorescence intensity varied notably across the three types of recharge water assessed. When *E. coli* cells dwell and grow in recharge ponds containing recharge water, the different physiologic responses observed are likely to be induced by the different levels of nutrient deprivation in different recharge water resources.

2.3 Strain and culturing methods

E. coli (ATCC25922) colonies were inoculated into 20 mL of Luria-Bertani (LB) medium (Sigma, Shanghai) and shaken at 150 r/min and 37°C for 6 h. Then the cells suspension at a volume ratio of 1:100 was incubated in LB medium for 16 h at 37°C. The cells were harvested by centrifugation (4000 × g, 10 min) and washed twice with sterilized DI water for complete removal of the LB medium prior to further analyses. Washed cells were then resuspended in DI water to obtain a concentration of 0.34–3.60 × 10^8 CFU/mL, as determined by optical density (OD_{600}) (UNICO 2800UV/VIS, USA) and confirmed by plate count analysis. The growth curve of *E. coli* is shown in Fig. S2. The standard curve of OD_{600} value and concentration of *E. coli* cells, as confirmed by plate counts, is shown in Fig. S3.

To study the influence of cell stagnation in recharge ponds/basins prior to infiltration, antecedent growth was

Main water quality parameters	LB medium	Rainfall	River water	SE
TOC (mg/L)	6858.50±16.50	0.28±0.04	5.25±0.68	7.53±1.02
COD (mg/L)	356.33±34.97	2.47±0.13	10.37±0.71	18.43±0.83
pH	7.00	7.05	7.63	7.68
TN (mg/L)	163.3±0.00	0.97±0.00	2.51±0.00	11.86±0.00
TP (mg/L)	6.08±0.00	0.004±0.00	0.13±0.00	0.04±0.00
IS (mM)	– –	0.35	4.87	7.66
Na^+ (mg/L)	– –	0.99	30.51	77.04
Mg^{2+} (mg/L)	– –	0.07	10.77	11.93
K^+ (mg/L)	– –	1.15	5.9	17.01
Ca^{2+} (mg/L)	– –	3.22	67.87	104.93
HCO_3^- (mg/L)	– –	23.72	172.75	203.79
Cl^- (mg/L)	– –	3.98	39.62	89.18
SO_4^{2-} (mg/L)	– –	0.81	19.77	25.84

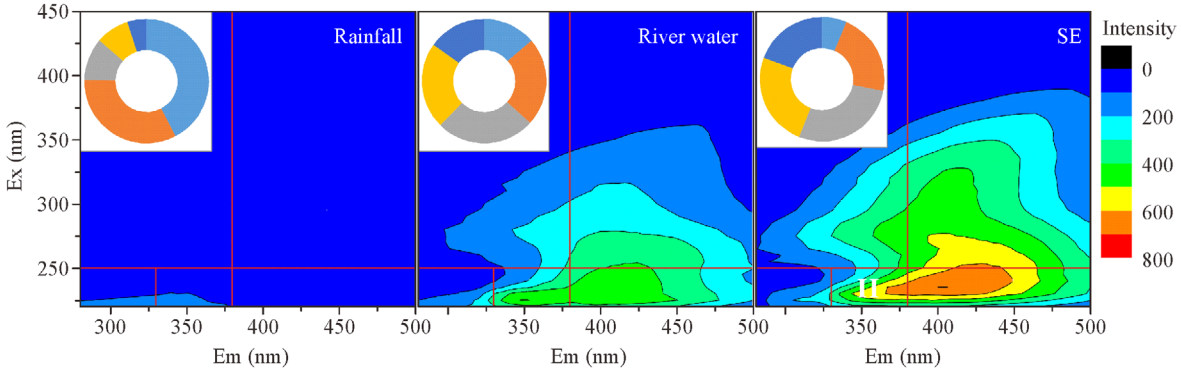

Fig. 1 Water quality parameters of the three types of recharge water and their 3DEEM spectra.

simulated for *E. coli* in recharge ponds, by suspending washed cells in recharge water solutions (rainfall, river water or SE) and incubating the solutions for 50 h. Following this, *E. coli* cells were used for characterization and transport experiments. The duration of 50 h was selected for simulated wet–dry cycle models of AGR operation, as the duration of wetting cycles is usually 1–3 days and the following drying cycles can also last several days (Ma et al., 1997; Karimi et al., 1998; Kallali et al., 2013). Therefore, 50 h cycles are equivalent to an approximate 2 day hydraulic retention period for bacteria in recharge ponds before infiltration, which is similar to previously reported real-world scenarios (Ma and Spalding, 1997; Karimi et al., 1998). An overview of the conceptual model is provided in Fig. 2.

2.4 Sand and bacterial characterization

Scanning electron microscopy (SEM) (XL30-ESEM, USA) was employed to observe the morphology of sand grains and *E. coli* cells, while their electrokinetic properties were measured using a zeta-potential tester (Nano-ZS, Malvern Instruments, UK). The hydrophobicity of *E. coli* cells was inferred from water contact angle measurement (OCA-20, DataPhysics Instruments, Germany). The cation exchange resin (CER) method was used to extract extracellular polymeric substances (EPS) of *E. coli* cells, which were quantified as the sum of total proteins and polysaccharides concentrations (Li et al., 2018). The concentrations of polysaccharides and proteins (mg/g cells) in EPS, were measured using the phenol-sulfuric acid method and the Bradford method, respectively (Li et al., 2018). In addition to the EPS content, outer membrane proteins (OMPs) have been reported to influence bacterial adhesion by altering cell surface properties (e.g., hydrophobicity). Many bacteria exhibit coordinated protective mechanisms to overcome these stresses and it is believed that the acquisition of cross protection during starvation is accomplished by the expression of starvation-stress proteins (Chourabi et al., 2017). In the present study, OMPs were extracted from *E. coli* cells and profiled using sodium dodecyl-sulfate polyacrylamide gel electrophoresis (SDS-PAGE), pre- and post-cultivation in recharge water solutions. The detailed procedure is outlined in S2 in Supplementary Material. The functional groups in *E. coli* extracellular macromolecules were characterized by Fourier transform infrared spectroscopy (FTIR) (Nicolet 6700 FTIR spectrometer, Thermo Fisher, USA).

2.5 Column experiments

Clean sand grains were wet-packed into acrylic columns (2.3 cm diameter and 11.3 cm height) to simulate the

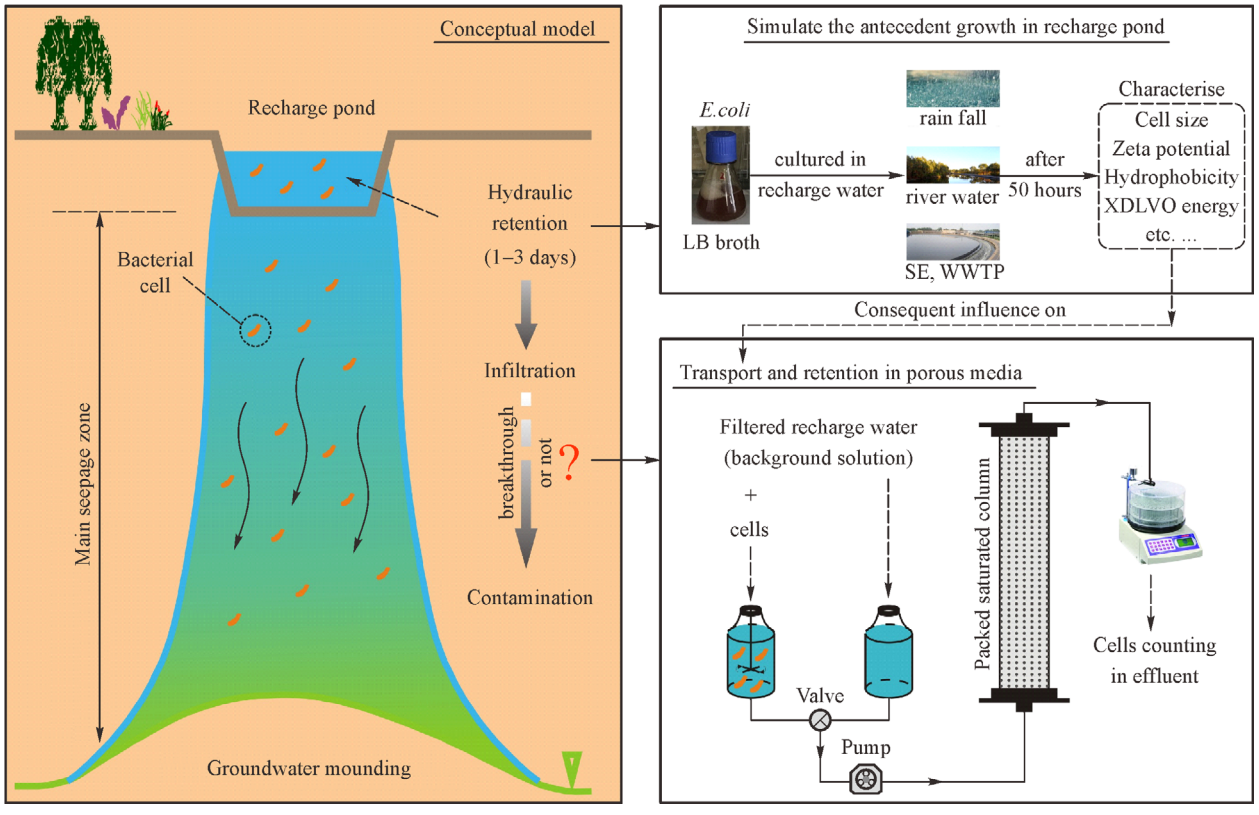

Fig. 2 The conceptual model and experimental design used in this study.

saturated seepage zone in an AGR system. The dimensions of the column used here were based on the column setup in several previous reports (Wang et al. 2012; Bradford et al. 2015; Banzhaf and Hebig, 2016; Chen et al. 2018; Ye et al. 2019). The acrylic columns were disinfected by ozonation for 20 min prior to transport experiments. The porosity of the packed column was 1.58±0.04 g/cm^3. All column experiments were performed in up-flow mode for saturated condition control at a stable flow rate of 2.80 mL/min using a peristaltic pump at 19.21±2.78°C, with duplicate analysis performed to verify the criterion of repeatability.

To examine the influence of antecedent growth on the physiologic states of *E. coli* cells in different recharge water resources, and the influence on cell transport, seven sets of experiments were performed (Table 1). Before *E. coli* suspensions were injected into the sand column, each column was flushed with the background electrolyte solution for 15 pore volumes (PVs) to achieve full equilibration. Then 4 PVs of *E. coli* suspension (C_0 = 2 × 10^8 CFU/mL) in the same background electrolyte composition were injected into the column (phase 1), followed by elution with the *E. coli*-free background electrolyte solution (~6 PVs) (phase 2). Effluent samples were collected every 2 min using a fraction collector (CBS-A 100, Huxi Company, China) to allow analysis of *E. coli* cell concentrations via the plate count method. Br^- was added to suspensions as a non-sorbing tracer, to track the breakthrough flow through soil columns and to estimate the hydraulic dispersion coefficient (D). The OD_{600} of the influent samples remained nearly constant (0.43±0.03) during transport experiments, indicating that the inflow boundary conditions were stable. After phase 2, the columns were destructively sampled to measure the amount of microbial deposition in the packed sand. The cell number desorbed per gram of sand in each 1 cm section, was normalized to the total cell number injected at phase 1 and the distribution along the column was demonstrated as the retention profile (1/g (%)) (Li et al., 2018). The total effluent mass retention ratio (R_r) was calculated by integrating the BTCs based upon the specified mass input of *E. coli* cells.

2.6 Interaction energy calculation and transport modeling

The cells-sand particles interaction energies were examined under different solution conditions, according to the extended Derjaguin Landau Verwey Overbeek (XDLVO) theory (Li et al., 2018; Yan et al., 2019). Detailed information on XDLVO calculations is provided in S3 in Supplementary Material. One dimensional advection-dispersion-retention equations were used to describe the transport process of *E. coli* cells in the saturated sand columns (Fan et al., 2015; Chu et al., 2019). This model can describe multiple mechanisms of cells transport, including advection, dispersion, straining, blocking and attachment/detachment (Bradford et al., 2003; Zhou et al., 2016), which are described in S4 in Supplementary Material.

3 Results and discussion

3.1 Cell morphology and electro-kinetic properties

During the 50 h cultivation period, *E. coli* cell populations did not vary obviously with cultivation time under all conditions investigated and OD_{600} values remained constant at around 0.55–0.65 (Fig. 3). Therefore, although cells survived for 50 h, they did not multiply massively in oligotrophic recharge water solutions. The morphological alterations of *E. coli* after growth in the three types of recharged water are shown in Fig. 3. SEM imaging showed that *E. coli* cells maintained their rod shape under all conditions. A considerable increase was observed in the apparent roughness of the outer surface of cells, with clearly visible wrinkles, which may be due to the tendency for bacteria to enlarge their specific surface area as a starvation response so that the nutrients can be transported into cells with minimum energy consumption (Sanin et al., 2003). The initial hydrodynamic diameter of *E. coli* cells ranged from 1.48 to 1.49 μm and decreased to 1.08–1.25 μm after starvation. The final average cell diameters after 50 h in various recharge water resources, were ranked

Table 1 Operational conditions for all column experiments

Expt. No.	Medium 1	Medium 2	IS (mM)	n (–)	D (cm^2/min)
1	LB broth	DI water	0	0.414	0.220
2	SE	DI water	0	0.423	0.298
3	River water	DI water	0	0.424	0.252
4	Rainfall	DI water	0	0.415	0.285
5	SE	SE	7.66	0.422	0.269
6	River water	Surface water	4.87	0.421	0.225
7	Rainfall	Rainfall	0.35	0.424	0.260

Note: Medium 1 was used for antecedent cultivation prior to transport column experiments, while medium 2 was applied as the background electrolyte solution in transport column experiments. IS was the ionic strength of medium 2.

in the descending order of SE (1.25±0.04 μm)>river water (1.14±0.12 μm)>rain fall (1.08±0.15 μm). Although only slight differences were observed, the order was consistent in all duplicated experiments. Considering that this intensity-weighted hydrodynamic diameter is relevant to the Brownian motion of suspended particles in liquid solutions (Ishii et al., 2010), these results indicate that the stability of cell suspensions increases in the sequence SE < river water < rainfall. Therefore, *E. coli* cells in SE should be the most aggressive to induce coagulation and deposition in the aquatic environment. Cell stability was further illustrated by the surface electrical properties of cells (Fig. 3). The zeta potential values of cells after 50 h of cultivation in SE, river water and rainfall were –21.4 ±3.95, –23.2±4.27 and –27.3±4.31 mV, respectively. After transferring the cells from LB medium or three recharge water types into DI water, the zeta potentials were –14.63±0.58, –23.3±3.4, –24.3±4.33 and –31.2±4.53 mV, respectively. The zeta potentials of sand particles were –18.7±0.96, –20.8±0.61, –24.9±0.74 and –32.0±1.2 mV in SE, river water, rainfall and DI water, respectively. Both the *E. coli* cells and sand particles were negatively charged, with the electronegative cell surfaces attributed to deprotonation of the O-functional groups, while electronegativity in quartz sand was due to dissociation of protons from silanol groups (i.e. SiOH) (Fan et al., 2015; Li et al., 2018). Although only slight change in zeta potential was observed among all experimental conditions, both the sand particles and cells were more electronegative in rainfall followed by river water and least electronegative in SE, showing good consistency in all water resources (Fig. 3). Zeta potential is considered to be affected by solution pH,

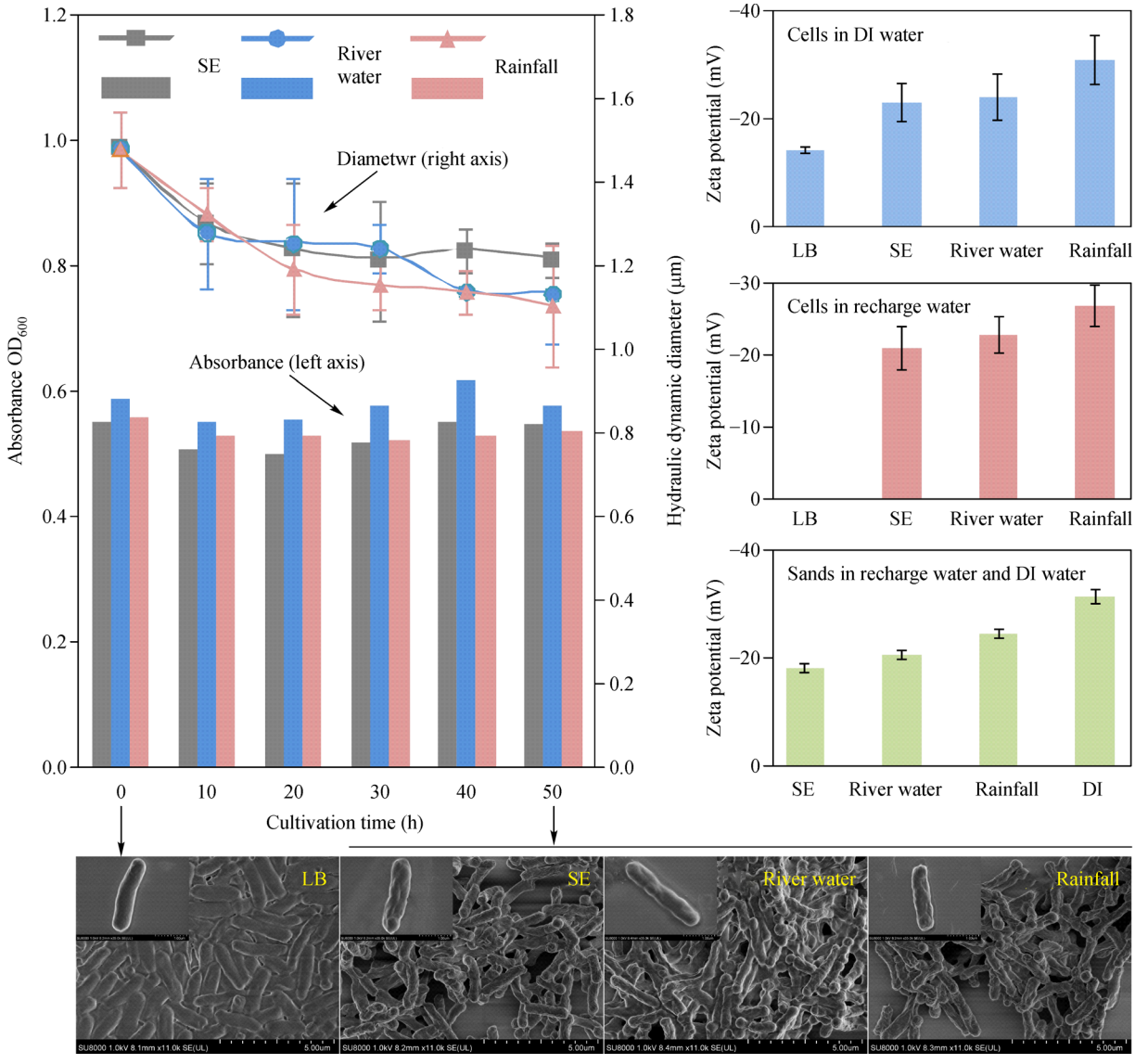

Fig. 3 Variation in OD_{600} and hydraulic dynamic diameter during the cultivation of *E. coli* in different recharge water resources, zeta potential of cells and sand particles, and SEM images of the cells pre- (LB medium) and post-cultivation for 50 h, under starvation conditions.

especially the concentration of counter-ions and coexisting organics (Fan et al., 2015). The pH variation range was relatively small in this study (7.05–7.68) and thus the influence of pH on the variation of zeta potential is quite low for the same IS (Walczak et al., 2012). Therefore, the difference in zeta potential in different water solutions observed in the present study could be attributed to compression of diffuse double layers around charged surfaces, due to the increased IS and charge neutrality because of coexisting cations (Fan et al., 2015). Furthermore, the zeta potential of colloid is more negative with increasing concentrations of coexisting organics (e.g., humic acid and fulvic acid) (Wang et al., 2012). As the content of organics detected in the recharge water was ranked in the descending order of SE>river water>rainfall, the influence of IS and cations on zeta potential was partly counterbalanced by the organics. Therefore, the differences in zeta potential were insignificant among all experimental conditions. The negative zeta potentials of the cells and sand particles result in strong repulsive electrostatic interactions, creating an unfavorable deposition interface between them.

3.2 Characterization of EPS and surface hydrophobicity

The results of EPS analysis using the CER method are shown in Fig. 4. The contents of proteins and polysaccharides, for *E. coli* cells in LB medium before cultivation in the three recharge water solutions were 77.95±3.65 and 14.41±0.18 μg/mg, respectively. *E. coli* cells cultivated in SE, river water and rainfall for 50 h, displayed protein contents of 43.01±4.51, 40.32±1.47, and 37.01±1.49 and carbohydrate contents of 12.68±0.61, 7.86±0.61, and 5.39±0.52 μg/mg, respectively. Therefore, the EPS of *E. coli* consisted mostly of proteins and the total EPS mass decreased sharply after starvation in recharge water solutions. Although the differences in EPS contents in different recharge water were not significant, the concentrations of both proteins and polysaccharides consistently followed the descending order of SE>river water>rainfall. The key functions of EPS comprise mediation of the initial attachment of cells to different substrata and protection of cells against environmental stress. If *E. coli* cells are unable to obtain enough external carbon/energy sources, EPS can be consumed. This may account for the decline in EPS in recharge water with a low DOC (0.28–7.53 mg/L). It has previously been reported that the presence of EPS on cell surfaces enhances cell deposition on silica surfaces, as compared to bio-particles with lower EPS contents (Tong et al., 2010; Lin et al., 2017). Therefore, the most severe retention of *E. coli* in sand columns would be induced by SE containing the maximum observed EPS concentrations.

The contents of proteins in total EPS mass in the three cultivation regimes were 43.01±4.51 in SE, 40.32±1.47 in river water and 37.01±1.49 μg/mg in rainfall. Several previous studies have reported that proteins were the key hydrophobic constituents of EPS, with cell hydrophobicity increasing according to the protein content (Liu and Fang, 2003; Li et al., 2018). This theory was verified by the contact angle results in the present study. The contact

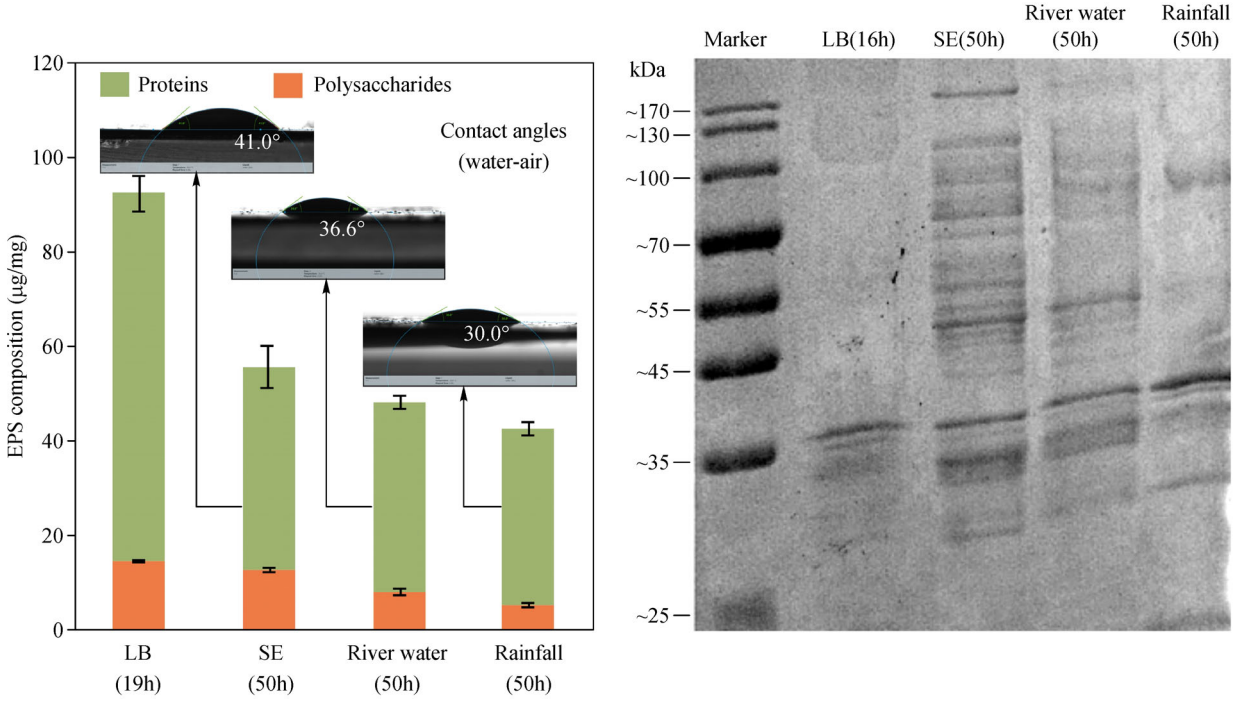

Fig. 4 EPS compositions, contact angles and OMP profiles for *E. coli* cells cultivated in different media (LB, SE, river water and rainfall).

angles (water phase) of *E. coli* cells cultivated in SE, river water and rainfall were 41.0°, 36.6° and 30.0°, respectively. Cells cultured in SE contained the largest amount of EPS and proteins, resulting in the highest hydrophobicity of all conditions assessed. Conflicting reports have shown that starvation can increase or decrease bacterial surface hydrophobicity, with both scenarios being ecologically viable (Liu and Fang, 2003; Li et al., 2018). In the present study, cell hydrophobicity decreased after starvation under all conditions, compared with the initial contact angle of 47.8° for cells cultivated in LB medium. Higher cell hydrophobicity could result in an increased affinity with the solid phase and relatively high attachment coefficient at the interface. This effect of hydrophobicity on bacterial adhesion can be explained by the decrease in surface free energy, in accordance with increasing hydrophobicity (Huang and Nitin, 2017). Therefore, cells with higher hydrophobicity exhibit a higher adsorption energy and ability to attach on sand surfaces.

The change in surface properties could also be attributed to the expression of coordinated protective bacterial mechanisms, to overcome multiple physical stresses. It has been previously reported that self-protection responses to starvation, are accomplished by the expression of starvation-stress proteins (Chourabi et al., 2017). In the present study, changes in cell surface proteins were examined by SDS-PAGE before starvation (cultivated in LB for 16 h) and after 50 h of cultivation in three types of recharge water, under starvation conditions. The major cell surface protein present under standard growth conditions (LB) was 35 kDa in size, with cells in recharge water maintaining this initial OMP. As shown in Fig. 4, the formation of new proteins occurred under all starvation condition regimes. For example, new bands were observed with sizes of 45, 70, 100 and 170 kDa in the OMP profiles (Fig. 4). Similar patterns were observed in all water resource scenarios, while the OMP of cells in SE were the most diverse, followed by those in river water and finally, rainfall. Although definitive conclusions cannot be drawn on whether the patterns of OMP changes can explain the variations in EPS, electrokinetic properties and hydrophobicity, alterations in OMP profiles were observed and the differences were significant. Sometimes, OMP profiling data are easier to interpret after long-term starvation, as the expression of these proteins is increased (Castellanos et al., 2000).

3.3 Influence of different cultivation regimes on transport of *E. coli* in DI water

The BTCs from experiments 1-4 are shown as normalized C/C_0~PV curves in Fig. 5. In experiments 1–4, the *E. coli* cells cultivated from LB, SE, river water and rainfall were washed and resuspended in DI water, before being fed into the sand columns. As the IS was maintained at a constant level by using DI water as the background solution, the influence of surface characteristics on cell transport could be specifically investigated. The maximum C/C_0 ($(C/C_0)_{max}$) values observed in experiments were 0.95 (rainfall-cells), 0.86 (river water-cells) and 0.82 (SE-cells). Since almost no cells were detected in effluents after 8 PVs, the calculated R_r values were expected to be reliable and were equal to 1.79% in rainfall-cells, 8.75% in river water-cells and 11.01% in SE-cells (Fig. 5). In contrast, the $(C/C_0)_{max}$ and R_r were 0.75 and 25.09% for LB-cells, respectively. This trend is in agreement with the aforementioned examination of surface characteristics. *E. coli* cells with larger hydraulic dynamic diameters, higher amounts of EPS and stronger hydrophobicity, displayed more severe retention within the sand column. The R_r of SE-cells was 9.22% greater than that of rainfall-cells and 14.08% less than that of LB-cells. Taken together, antecedent growth of *E. coli* in insufficient nutrient recharge pond environments before infiltration, resulted in cell starvation and changed the physiologic state of cells, increasing their mobility in porous media. The dashed lines in Fig. 5 indicate the model fitting results, exhibiting a reasonable fit for all experimental BTCs ($R^2>0.95$). The k_{det} values in all experiments were less than 0.001 and were far below the equivalent k_{att} values. In addition, no tailing was observed in any BTCs, indicating that the remobilization of previously deposited cells was insignificant. In experiments 1–4, the average k_{att} values were 0.316, 0.189, 0.163 and 0.092 min^{-1} for LB-cells, SE-cells, river water-cells and rainfall-cells, respectively. This modeling result was in agreement with the $(C/C_0)_{max}$ and R_r values, as well as being consistent with the results of surface properties analyses.

3.4 Transport of *E. coli* during AGR with the three types of recharge water

The BTCs of *E. coli* cells in experiments 5–7 are shown in Fig. 6. In these experiments, *E. coli* cells were cultivated in SE, river water and rainfall for 50 h before suspensions were fed into the columns. After long-term operation of AGR systems, the hydro-chemical conditions in recharge basins/ponds and the seepage zone were highly similar. Therefore, the same conditions were maintained for medium 1 and medium 2 (Table 1) to simulate the actual situation in field AGR sites. The $(C/C_0)_{max}$ was 0.94 in rainfall, 0.84 in river water and 0.72 in SE, while the R_r values were 2.70%, 10.38% and 16.93%, respectively. The corresponding k_{att} values were 0.078, 0.149 and 0.286, respectively. The *E. coli* cells in rainfall displayed the highest mobility, followed by river water and finally SE, showing the lowest mobility. These findings show a reverse trend to the pattern of IS for the three types of recharge water. Cells in SE with the higher IS and cation concentrations (e.g., Ca^{2+}, Mg^{2+} in Fig. 1) displayed the most severe retention in the column. These findings also conform to the electrical double layer compression effect

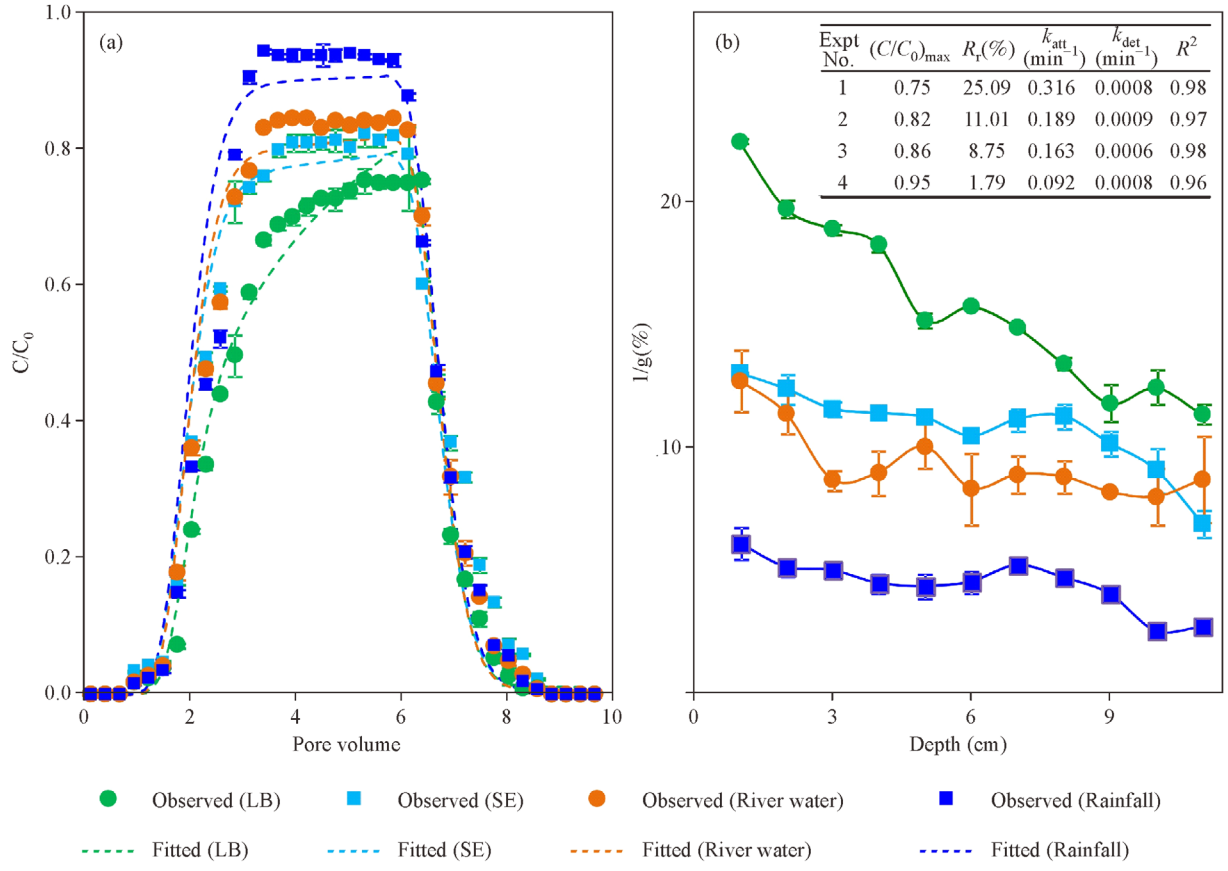

Fig. 5 Breakthrough curves (a) and retention profiles (b) for *E. coli* cells cultivated in different media (LB, SE, river water and rainfall), with distilled-deionized water used as the background electrolyte solution (Experiments No. 1–4).

induced by increasing the IS (Fan et al., 2015; Ye et al., 2019). The compression of diffuse double layers could result in a reduction in repulsive forces between cells and sand particles. It was also observed that there were several types of coexisting divalent cations in recharge water, which can usually be bound by carboxylic or hydroxyl groups on the cell surface, forming bridges that can enhance cell aggregation. However, slight variation in the hydrodynamic diameter of cells in different recharge waters (section 3.1) indicated that cationic bridging is not the dominant retention mechanism.

Unlike the relatively high IS (10 to 1000 mM) conditions reported in previous studies (Yang et al., 2013; Zhou et al., 2016; Ye et al., 2019), the IS of different recharge water resources determined in the present study only varied from 0.35 to 7.66 mM, which is typical for freshwater conditions in actual AGR systems. According to the aforementioned results, if recharge water is mixed with rainfall or river water, the mobility of *E. coli* cells is greater, presenting a higher risk of potential contamination of underlying groundwater with pathogenic microbes. In contrast, the retention of *E. coli* cells is significantly improved in AGR with SE. This results in accumulation of cells in porous media and damage to the sand matrix (clogging), creating a potential hotspot for pollutant release (Perujo et al., 2019). In addition, the influence of IS in these experiments implies that the trapped *E. coli* cells could be re-released from the sand matrix after dilution events, such as elution by rainfall with a lower IS (Zhu et al., 2019), resulting in a concentrated pulse of *E. coli* cells being released.

3.5 *E. coli* transport and deposition mechanisms during the simulated AGR process

All BTCs in this study showed some retention in breakthrough compared to the tracer Br^- with the possible mechanisms including straining, blocking and attachment/detachment. As the diameter ratios of *E. coli* cells to sand particles are within the range of 0.002–0.003, straining is unlikely to occur as the ratios are less than the threshold values (0.005 and 0.008) proposed by previous studies (Xu et al., 2006; Johnson et al., 2007). This theory is also supported by the non-hyperexponential distribution of retained cells along the column (Figs. 5(b) and 6(b)). Therefore, straining is not likely to be significant to the retention mechanism. Blocking usually results in previously deposited cells hindering subsequent deposition,

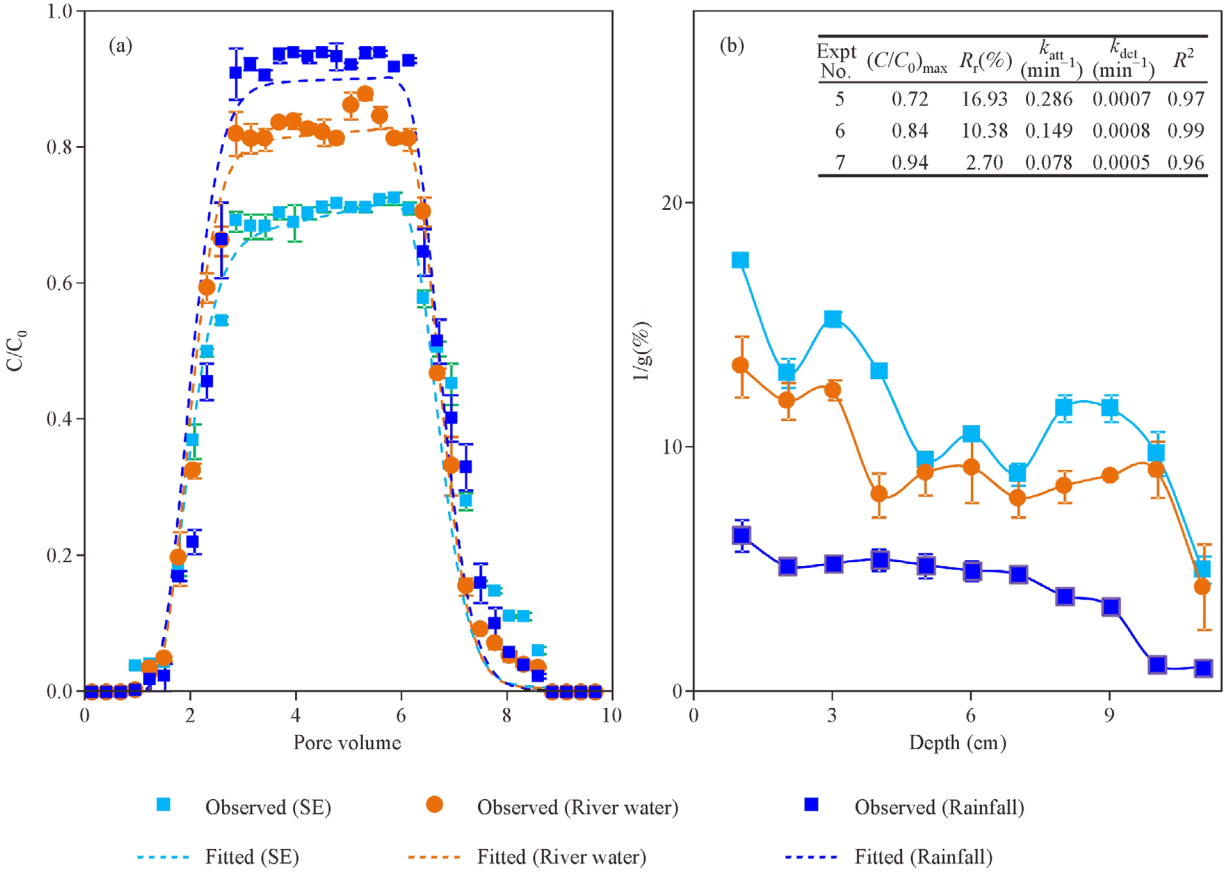

Fig. 6 Breakthrough curves (a) and retention profiles (b) for *E. coli* cells cultivated in different media (SE, river water and rainfall), with the equivalent medium subsequently used as the background electrolyte solution in columns (Experiments No. 5–7).

causing a continual increase in cell concentrations in the effluent. However, all BTCs exhibited mostly symmetric curves which flattened after 2.86 PVs, implying the absence of blocking effects in this study.

As shown in section 3.1, under all experimental conditions in this study unfavorable deposition interfaces were formed between the electronegative *E. coli* cells and sand particles. The calculations based on XDLVO theory predicted the presence of substantial repulsive energy barriers greater than 6000 k_BT under all scenarios, making it difficult for cells to overcome the energy barrier and deposit on sand particle surfaces at the primary energy minimum. Taking the results of experiments 5–7 as examples (Fig. 7), inspection of the contributions of VDW, EDL and AB forces indicated that the strong repulsive AB force was significantly higher than the generally repulsive EDL force and was primarily responsible for the magnitude of the energy barrier at short distances. However, a secondary energy minimum (Φ_{min}) existed at distances greater than the repulsive barrier in all XDLVO curves. The depths of the Φ_{min} were $-4.16 \times 10^{-5} k_BT$ at 82 nm in rainfall, $-4.83 \times 10^{-5} k_BT$ at 78 nm in river water and $-8.75 \times 10^{-5} k_BT$ at 61 nm in SE. The secondary energy minimum was attributed to the negative LW force, which was 1–3 orders of magnitude greater than the EDL force. The AB force decreased sharply with increasing distance and therefore, exerted an insignificant impact on the Φ_{min}. Higher (or deeper) Φ_{min} values have been reported to increase deposition, probability at the secondary minimum where favorable deposition conditions are represented (Hori and Matsumoto, 2010). Therefore *E. coli* cells within SE are the most likely to deposit on the sand surface, which is in good agreement with the experimental results of the present study.

Although the apparent zeta potential of both particles was negative, positive sites remain on their surfaces due to surface charge heterogeneities, which may create locally favorable retention sites. The surface charge heterogeneity of mineral grains has been used to explain the weak retention of nanoparticles in soil column under low IS conditions (Ollivier et al., 2018). Furthermore, several different types of charged functional groups are present in the EPS of *E.coli*, such as hydroxyl, carboxyl, amide and aldehyde groups (Lu et al., 2011). Additionally, as the main component of EPS in this study, proteins usually contain positive functional groups (e.g., amino groups). This was

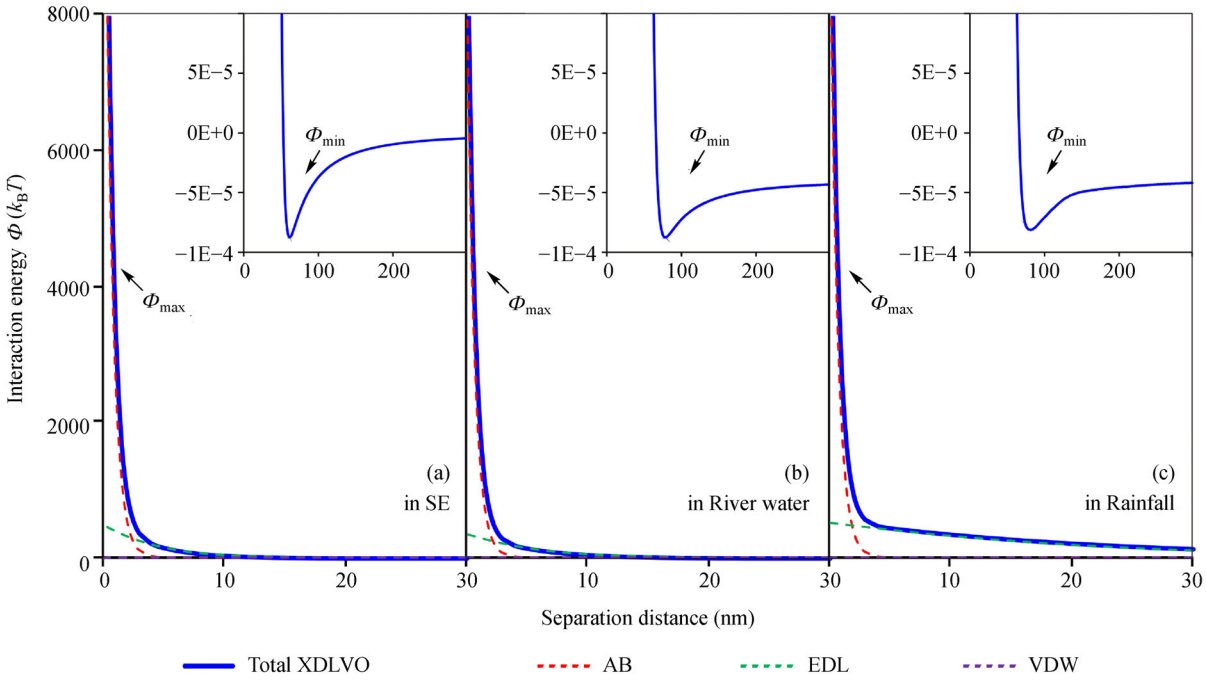

Fig. 7 XDLVO energy profiles for interactions between sand particles and *E. coli* cells cultivated in different recharge water matrices.

verified by FTIR analysis of *E.coli* cells cultivated in LB medium, as shown in Fig. S4. The bands observed at 1636 cm^{-1}, 1541 cm^{-1} and 1219 cm^{-1} were attributed to amide I, amide II and amide III vibration in proteins, respectively. These positive charged amino groups can provide favorable deposition sites for negative sand particles and can neutralize the negative charges of carboxyl and phosphate groups, decreasing the net negative surface charges of cells (Sheng et al., 2010; Kumar et al., 2016) and accounting for the negative effect of proteins on net surface charges. In the present study, cell starvation led to a decrease in protein content, causing cells to become more negatively charged.

Admittedly, all mechanisms discussed in this section might be limited to the scale of the experiment and not directly transferrable to field scales as many parameters are exclusive to the column setup. For example, the saturation condition could vary from unsaturated to saturated one, and there may be water-rock interaction during the ASR. All these factors could affect the behavior of *E. coli* in porous medium. Nevertheless, this study shows how the antecedent growth process in spreading pond alters characteristics of *E. coli*, and provides insight into the transport behavior of *E. coli* through saturated porous media with different real recharge water types. The results are particularly useful for long-running ASR sites shaving stable system with water-rock interaction equilibrium.

4 Conclusions

In AGR systems, the dwelling process of different recharge water types (SE, river water and rainfall) in recharge ponds, induces physiologic stress on *E. coli* cells, as the commonly used recharge water sources are generally oligotrophic (low nutrients) with low ionic strengths and different cationic compositions. In this study, the antecedent growth in three types of real recharge water was simulated in laboratory scale experiments. The results demonstrated that this process led to changes in cell properties, such as size, zeta potential, EPS, outer membrane protein profiles and surface hydrophobicity. After cultivation in recharge water for 50 h, the zeta potential of *E. coli* cells became more negative, with reduced hydrodynamic diameters, decreased EPS concentrations and surface hydrophobicity, while the OMP of cells became more diverse. These responses influenced *E. coli* transport in subsurface environments, with *E. coli* cells in rainfall displaying the highest mobility (least retention), followed by river water cells and SE cells (most retention). The results of interaction energy calculations and transport modeling provide quantitative support for the experimental results. Admittedly, the biological driving mechanisms accounting for the changes in cells properties in recharge ponds require further investigation to fully understand the role of antecedent growth. Overall, this study demonstrated the transport of *E. coli* in different recharge water types during simulated AGR, furthering our understanding and providing a basis to assess the spreading risk of pathogenic microbes in practical AGR applications. Nevertheless, the combined effects of other factors (e.g., water-rock interaction, soil heterogeneity, and unsaturated condition) on the *E. coli* transport are still require further study.

Acknowledgements This work was funded by the National Natural Science Foundation of China (Grant Nos. 51678121, 51978135, and 41772236). It was also supported by "the Fundamental Research Funds for the Central Universities, China" (No. 2412019ZD004).

Electronic Supplementary Material Supplementary material is available in the online version of this article at https://doi.org/10.1007/s11783-020-1242-0 and is accessible for authorized users.

References

Amimi A S H A, Khan M A, Dghaim R (2014). Bacteriological quality of reclaimed wastewater used for irrigation of public parks in the United Arab Emirates. International Journal of Environmental Science and Development, 5: 309–312

Asanoa T, Cotruvo J A (2004). Groundwater recharge with reclaimed municipal wastewater: Health and regulatory considerations. Water Research, 38: 1941–1951

Banzhaf S, Hebig K H (2016). Use of column experiments to investigate the fate of organic micropollutants: A review. Hydrology and Earth System Sciences, 20(9): 3719–3737

Bouwer H (2002). Artificial recharge of groundwater: Hydrogeology and engineering. Hydrogeology Journal, 10: 121–142

Bradford S A, Headd B, Arye G, Šimůnek J (2015). Transport of *E. coli* D21g with runoff water under different solution chemistry conditions and surface slopes. Journal of Hydrology, 525: 760–768

Bradford S A, Simunek J, Bettahar M, Van Genuchten M T, Yates S R (2003). Modeling colloid attachment, straining, and exclusion in saturated porous media. Environmental Science & Technology, 37: 2242–2250

Cai P, Huang Q, Walker S L (2013). Deposition and survival of *Escherichia coli* O157:H7 on clay minerals in a parallel plate flow system. Environmental Science & Technology, 47: 1896–1903

Castellanos T, Ascencio F, Bashan Y (2000). Starvation-induced changes in the cell surface of *Azospirillum lipoferum*. FEMS Microbiology Ecology, 33: 1–9

Chen F, Yuan X, Song Z, Xu S, Yang Y, Yang X (2018). Gram-negative *Escherichia coli* promotes deposition of polymer-capped silver nanoparticle in saturated porous media. Environmental Science: Nano, 5: 1495–1505

Chen W, Westerhoff P, Leenheer J A, Booksh K (2003). Fluorescence excitation-emission matrix regional integration to quantify spectra for dissolved organic matter. Environmental Science & Technology, 37: 5701–5710

Chourabi K, Torrella F, Kloula S, Rodriguez J A, Trabelsi I, Campoy S, Landoulsi A, Chatti A (2017). Adaptation of Shigella flexneri to starvation: morphology, outer membrane proteins and lipopolysaccharide changes. Arabian Journal of Geosciences, 10: 274–280

Chu T, Yang Y S, Lu Y, Du X Q, Ye X Y (2019). Clogging process by suspended solids during groundwater artificial recharge: Evidence from lab simulations and numerical modelling. Hydrological Processes, doi: 101002/hyp13553

Dillon P (2005). Future management of aquifer recharge. Hydrogeology Journal, 13: 313–316

Dwivedi D, Mohanty B P, Lesikar B J (2013). Estimating *Escherichia coli* loads in streams based on various physical, chemical, and biological factors. Water Resources Research, 49: 2896–2906

Engström E, Thunvik R, Kulabako R, Balfors B (2014). Water transport, retention, and survival of Escherichia coli in unsaturated porous media: A comprehensive review of processes, models, and factors. Critical Reviews in Environmental Science and Technology, 45(1): 1–100

Fan W, Jiang X H, Yang W, Geng Z, Huo M X, Liu Z M, Zhou H (2015). Transport of graphene oxide in saturated porous media: Effect of cation composition in mixed Na-Ca electrolyte systems. Science of the Total Environment, 511: 509–515

Foppen J W A, Schijven J F (2006). Evaluation of data from the literature on the transport and survival of *Escherichia coli* and thermotolerant coliforms in aquifers under saturated conditions. Water Research, 40: 401–26

Goldberg E, Scheringer M, Bucheli T D, Hungerbühler K (2014). Critical assessment of models for transport of engineered nanoparticles in saturated porous media. Environmental Science & Technology, 48: 12732–12741

Hao R, Ren H, Li J, Ma Z, Wan H, Zheng X, Cheng S (2012). Use of three-dimensional excitation and emission matrix fluorescence spectroscopy for predicting the disinfection by-product formation potential of reclaimed water. Water Research, 46: 5765–5776

Hori K, Matsumoto S (2010). Bacterial adhesion: From mechanism to control. Biochemical Engineering Journal, 48: 424–434

Huang K, Nitin N (2017). Enhanced removal of *Escherichia coli* O157: H7 and Listeria innocua from fresh lettuce leaves using surfactants during simulated washing. Food Control 79: 207–217

Ishii K, Iwai T, Xia H (2010). Hydrodynamic measurement of Brownian particles at a liquid-solid interface by low-coherence dynamic light scattering. Optics Express, 18: 7390–7396

Jalšenjak N (2006). Contribution of micelles to ionic strength of surfactant solution. Journal of Colloid and Interface Science, 293(1): 230–239

Johnson W P, Li X, Yal G (2007). Colloid retention in porous media: Mechanistic confirmation of wedging and retention in zone of flow stagnation. Environmental Science & Technology, 41: 1279–1287

Kallali H, Yoshida M, Tarhouni J, Jedidi N (2013). Generalization and formalization of the US EPA procedure for design of treated wastewater aquifer recharge basins: II Retrofit of Souhil Wadi (Nabeul, Tunisia) pilot plant. Water Science & Technology, 67: 764–772

Karimi A A, Redman J A, Ruiz R F (1998). Ground water replenishment with reclaimed water in the city of Los Angeles. Ground Water Monitoring and Remediation, 18: 150–158

Kumar G, Mudhoo A, Sivagurunath P, Nagaraj D, Ghimire A, Lay C H, Lin C Y, Lee, D J, Chang J S (2016). Recent insights into the cell immobilization technology applied for dark fermentative hydrogen production. Bioresource Technology, 219: 725–737

Levantesi C, La Mantia R, Masciopinto C, Böckelmann U, Ayuso-Gabella M N, Salgot M, Tandoi V, Van Houtte E, Wintgens T, Grohmann E (2010). Quantification of pathogenic microorganisms and microbial indicators in three wastewater reclamation and managed aquifer recharge facilities in Europe. Science of the Total Environment, 408: 4923–4930

Li Q, Yang J, Fan W, Zhou D, Wang X, Zhang L, Huo M, Crittenden J C (2018). Different transport behaviors of Bacillus subtilis cells and

spores in saturated porous media: Implications for contamination risks associated with bacterial sporulation in aquifer. Colloids and surfaces B: Biointerfaces, 162: 35–42

Lin D, Story S D, Walker S L, Huang Q, Liang W, Cai P (2017). Role of pH and ionic strength in the aggregation of TiO_2 nanoparticles in the presence of extracellular polymeric substances from *Bacillus* subtilis. Environmental Pollution, 228: 35–42

Liu Y, Fang H H P (2003). Influences of extracellular polymeric substances (EPS) on flocculation, settling, and dewatering of activated sludge. Critical Reviews in Environmental Science and Technology, 33: 237–273

Lopez-Galvez F, Gil M I, Pedrero-Salcedo F, Alarcón J J, Allende A (2016). Monitoring generic Escherichia coli in reclaimed and surface water used in hydroponically cultivated greenhouse peppers and the influence of fertilizer solutions. Food Control, 67: 90–95

Lu X, Liu Q, Wu D, Al-Qadiri H M, Al-Alami N I, Kang D H, Shin J H, Tang J, Jabal J M F, Aston E D, Rasco B A (2011). Using of infrared spectroscopy to study the survival and injury of *Escherichia coli* O157:H7, *Campylobacter jejuni* and *Pseudomonas aeruginosa* under cold stress in low nutrient media. Food Microbiology, 28: 537–546

Ma L, Spalding R F (1997). Effects of artificial recharge on ground water quality and aquifer storage recovery. Journal of the American Water Resources Association, 33: 561–572

Madumathi G (2017). Transport of *E. coli* in presence of naturally occuring colloids in saturated porous media. Water Conservation Science and Engineering, 2: 153–164

Mauter M, Fait A, Elimelech M, Herzberg M (2013). Surface cell density effects on *Escherichia coli* gene expression during cell attachment. Environmental Science & Technology, 47: 6223–6230

Ollivier P, Pauwels H, Wille G, Devau N, Braibant G, Cary L, Picot-Colbeaux G, Labille J (2018). Natural attenuation of TiO2 nanoparticles in a fractured hard-rock. Journal of Hazardous Materials, 359: 47–55

Pachepsky Y A, Shelton D R (2011). Escherichia coli and fecal coliforms in freshwater and estuarine sediments. Critical Reviews in Environmental Science and Technology, 41: 1067–1110

Perujo N, Romaní A M, Sanchez-Vilaab X (2019). A bilayer coarse-fine infiltration system minimizes bioclogging: The relevance of depth-dynamics. Science of the Total Environment, 669: 559–569

Sanin S L, Sanin D, Bryers J D (2003). Effect of starvation on the adhesive properties of xenobiotic degrading bacteria. Process Biochemistry, 38: 909–914

Sheng G P, Yu H Q, Li X Y (2010). Extracellular polymeric substances (EPS) of microbial aggregates in biological wastewater treatment systems: A review. Biotechnology Advances, 28: 882–894

Sherchan S, Miles S, Ikner L, Yu H, Snyder S A, Pepper I L (2018). Near real-time detection of *E. coli* in reclaimed water. Sensors 18, 2303–2312

Tong M P, Long G Y, Jiang X J, Kim H (2010). Contribution of extracellular polymeric substances on representative gram negative and gram positive bacterial deposition in porous media. Environmental Science & Technology, 44: 2393–2399

Walczak J J, Wang L, Bardy S L, Feriancikova L, Li J, Xu S (2012). The effects of starvation on the transport of Escherichia coli in saturated porous media are dependent on pH and ionic strength. Colloids and surfaces B: Biointerfaces, 90: 129–136

Wang D, Bradford S A, Harvey R W, Gao B, Cang L, Zhou D (2012). Humic acid facilitates the transport of ARS-labeled hydroxyapatite nanoparticles in iron oxyhydroxide-coated sand. Environmental Science & Technology, 46: 2738–2745

Wang Y, Huo M, Li Q, Fan W, Yang J, Cui X (2018). Comparison of clogging induced by organic and inorganic suspended particles in a porous medium: Implications for choosing physical clogging indicators. Journal of Soils and Sediments, 18: 2980–2994

Wang Z J (2012). Laboratory research on the law of suspended solids clogging during urban stormwater groundwater recharge. Dissertation for the Doctoral Degree. Changchun: Jilin University, 11–21 (in Chinese)

Xu S P, Gao B, Saiers J E (2006). Straining of colloidal particles in saturated porous media. Water Resources Research, 42: W12S16

Yan C, Chen T, Shang J (2019). Effect of bovine serum albumin on stability and transport of kaolinite colloid. Water Research, 155: 204–213

Yang J, Bitter J L, Smith B A, Fairbrother D H, Ball W P (2013). Transport of oxidized multi-walled carbon nanotubes through silica based porous media: Influences of aquatic chemistry, surface chemistry, and natural organic matter. Environmental Science & Technology, 47: 14034–14043

Ye X Y, Cui R, Du X, Ma S, Zhao J, Lu Y, Wan Y (2019). Mechanism of suspended kaolinite particle clogging in porous media during managed aquifer recharge. Groundwater, 57: 764–771

Zhou D D, Jiang X H, Lu Y, Fan W, Huo M X, Crittenden J C (2016). Cotransport of graphene oxide and Cu (II) through saturated porous media. Science of the Total Environment, 550: 717–726

Zhu L, Torres M, Betancourt W Q, Sharma M, Micallef S A, Gerba C, Sapkota A R, Sapkota A, Parveen S, Hashem F, May E, Kniel K, Pop M, Ravishankar S (2019). Incidence of fecal indicator and pathogenic bacteria in reclaimed and return flow waters in Arizona, USA. Environmental Research, 170: 122–127

Zhu Y G, Zhai Y Z, Du Q Q, Teng Y G, Wang J S, Yang G (2019). The impact of well drawdowns on the mixing process of river water and groundwater and water quality in a riverside well field, Northeast China. Hydrological Processes, 33: 945–961